Topics in Catalysis Vol. 38, No. 4, August 2006 (© 2006)
DOI: 10.1007/s11244-006-0025-6

Original Paper

Hybrid materials for immobilization of MP-11 catalyst

Thomas J. Pisklak, Minedys Macías, Decio H. Coutinho, Rita S. Huang, and Kenneth J. Balkus, Jr.*
Department of Chemistry and UTD Nanotech Institute, University of Texas at Dallas, Richardson, TX 75080-0688, USA

Microperoxidase-11(MP-11) has been immobilized for the first time in hybrid periodic mesoporous organosilica (PMO) materials and in a nano-crystalline metal organic framework (MOF). Microperoxidase-11 was physically absorbed from solution into the periodic mesoporous organosilica MBS and functionalized derivatives of MBS as well as in the 3-dimensional $[Cu(OOC–C_6H_4–C_6H_4–COO)\cdot ½\ C_6H_{12}N_2]_n$ metal organic framework. The conversion of Amplex® UltraRed and methylene blue to their respective oxidation products by immobilized MP-11 was determined.

KEY WORDS: immobilization; metal organic framework; microperoxidase-11; mesoporous materials; oxidation.

1. Introduction

Nature's catalysts, enzymes, exhibit chemically desirable properties which many in the field of catalysis strive to duplicate as well as undesirable properties. Enzymes are generally more active and selective catalysts while operating under milder conditions than corresponding biomimetic catalysts [1]. Also, enzymes exhibit high selectivity for reagent binding which promotes the synthesis of desired products over by-products. However, some of the undesirable properties of enzymes include low thermal stability, difficult recycling of catalyst, and low stability in organic solvents.

In efforts to replicate the desirable features of enzymes while overcoming the stability issues, zeolite enzyme mimics have been studied [1–8]. These biomimetic systems are based on the ability of zeolites to potentially differentiate molecules based on size and shape selectivity. Utilizing zeolites as a host matrix for an active site model provides the inherent thermal stability of zeolites which allows reactions to be carried out at higher temperatures while also allowing for a wider range of solvent systems. The encapsulation of homogenous catalysts in the pores of zeolites gave rise to the concept of ship-in-a-bottle catalysts. Zeolite enzyme mimics or zeozymes have been synthesized either by crystallizing the zeolite around the metal complex or by assembling the complex in the pores. In both cases the encapsulated metal complex catalyst should be too large to exit the pore windows of the zeolite. In the case of the synthesis method [9–12] transition metal complexes are placed in the synthesis gel and encapsulated during crystallization. This approach gives well defined guest molecules with homogeneous dispersions. Not only has higher catalyst activity and size selectivity been achieved with such systems but also higher enantioselectivity [9] relative to the homogenous analog. Higher loadings of catalyst can be obtained by ion exchange of preformed metal complexes in the zeolite [3], however, the metal complexes may be susceptible to leaching. The catalyst may be covalently attached to the zeolite by organosilanes [1] to overcome the leaching problem but the ligand may also attach to the exterior surface as well as the pore walls. This also reduces the size and shape selectivity of the zeolite host. In situ assembly of a catalyst inside the zeolite may be accomplished by several different methods. For example, we have previously described the flexible ligand method [8] in which the zeolite is first ion exchanged with a transition metal ion followed by diffusion of an organic ligand into the zeolite, forming the target metal complex that becomes too big to exit the pores. Alternatively, a transition metal exchanged zeolite can be exposed to a ligand precursor which can then condense in a template fashion to form the desired ligand and encapsulated complex. For example, phthalonitrile has been adsorbed onto a metal exchanged zeolite followed by intrazeolite condensation to form a metallophthalocyanine complex [10–12]. While the high selectivity and activity can be achieved with ship-in-a-bottle catalysts, so far nature still provides the most efficient catalysts for many reactions. The question then becomes, can one simply encapsulate an enzyme in a zeolite to enhance the stability of the biocatalyst? Unfortunately, most enzymes are much larger than the largest pore zeolite (1 nm). However, the discovery by Mobil of mesoporous molecular sieves such as MCM-41 presented the opportunity to support biocatalysts that would require 2–50 nm pore sizes.

The immobilization of small enzymes and proteins by absorption in mesoporous molecular sieves may offer many advantages over traditional methods of

* To whom correspondence should be addressed.
E-mail: balkus@utdallas.edu

biocatalyst immobilization such as covalent binding, membrane encapsulation, cross-linking, and sol–gel entrapment [13]. Mesoporous molecular sieves can be comprised of one- to three-dimensional channel systems and have uniform pores ranging from 2 to 50 nm. These host materials can be compositionally tailored to provide various desired properties such as hydrophobicity/hydrophilicity as well as surface binding sites. The uniform pore structure of mesoporous molecular sieves is an improvement over amorphous sol–gel derived materials that generally exhibit a fairly broad pore size distribution. The uniform pores of molecular sieve materials allow for control of molecular absorption on the basis of size. Confinement of the enzyme in a well-defined pore space may also help prevent protein denaturing. The mesoporous host materials are often chemically inert and stable at elevated temperatures. Additionally, the pore structure may be systematically varied, which may provide insight into changes in the tertiary structure and active site during catalysis. Balkus and Diaz [14] were the first to report the immobilization of enzymes in mesoporous materials. In this case, MCM-41 which has one-dimensional channels in a hexagonal array, was employed to immobilize cytochrome c, papain, and trypsin. Subsequently, other materials such as cubic MCM-48, SBA-15, and Nb-TMS-1 were also used by our group to immobilize cytochrome c [15]. A growing number of researchers have since immobilized various enzymes in a wide range of mesoporous materials [16–68], as shown in table 1. While most studies involve different types of mesoporous silica or mesoporous silica functionalized with organosilanes there are opportunities to expand the range of mesoporous materials to include inorganic/organic hybrid frameworks

We are now developing the next generation of enzyme host materials. These hybrid materials include: periodic mesoporous organosilicas (PMOs) [69] and functionlized PMOs such as mesoporous benzene silica (MBS) [70] (figure 1), aminopropyl-MBS (AP-MBS), ethylenediamine-MBS (EDA-MBS). The MBS material is prepared by the condensation of bis(triethoxysilyl)benzene (BTEB) around a surfactant template. The mesopores of this material are lined with periodically ordered benzene rings. Also, we report for the first time the immobilization of the microperoxidase MP-11 into a metal organic framework (MOF), figure 2. The CuMOF employed in this study was first synthesized by Seki *et al.* [71]. The MOF is comprised of copper dimers connected via 4,4′-biphenyldicarboxylates to form molecular squares, these are then connected through the copper by bridging ligands to form channels. Metal organic frameworks comprise a relatively new class of porous materials. MOFs are constructed from metal ions or metal clusters connected by bridging organic ligands to form a porous structure. MOF's have been shown to have some of the highest surface areas of known materials [72]. The 17.8 nm pores of the CuMOF should be able to adsorb small enzymes and proteins.

In the present study, microperoxidase-11 (MP-11), shown in figure 3, was selected for immobilization in the PMO and MOF materials. MP-11 is the product of proteolytic degradation of cytochrome c. The active site in this peroxidase involves an iron heme group. MP-11's

Table 1
Summary of enzymes and host materials used for immobilization

Enzyme	Host Materials	Reference
Acid Phosphatase (ACP)	Mesoporous Silica	[16–19]
α-Amylase	SBA-15, MCF-153, MCF-335A, MCM-41	[20–22]
Catechol Oxidase	MCM-41	[23]
Catalase	Mesoporous Silica Spheres (MSSs)	[24–25]
Chloroperoxidase	MCF, Mesoporous Silica	[26–27]
α-Chymotrypsin	MCM-41	[28]
Cytochrome c	MCM-41, FSM-16, SBA-15, NbTMS-1	[14, 25, 29–36]
Earthworm Serine Protease	FSM	[38]
β-Galactosidase	MCM-41	[39]
Glucose Oxidase	Aluminosilicates	[40–44]
Hemoglobin	HMS	[45]
Horsradish Peroxidase	FSM-16, MCM-41, SBA-15, Nb_2O_5	[32, 43, 44, 46–50]
Lipases	MCM-41, MCM-36, Mesoporous silica	[51–55]
Lysozyme	MCM-41, SBA-15	[56–59]
Manganese Peroxidase	FSM-16	[60]
Methane mono-oxygenase	HMS, MCM-41	[61]
Myoglobin	HMS	[62]
Organophosphorus Hydrolase (OPS)	Functionalized Mesoporous Silica (FMS)	[63]
Papain	MCM-41	[14]
Penicillin G Acylase	MCM-41, SBA-15	[64–65]
Protease	MSSs	[25]
Ribonuclease A	MCM-48	[66]
Subtilisin	FSM-16, MCM-41	[46]
Trypsin	SBA-15, MCM-41	[14, 67–68]

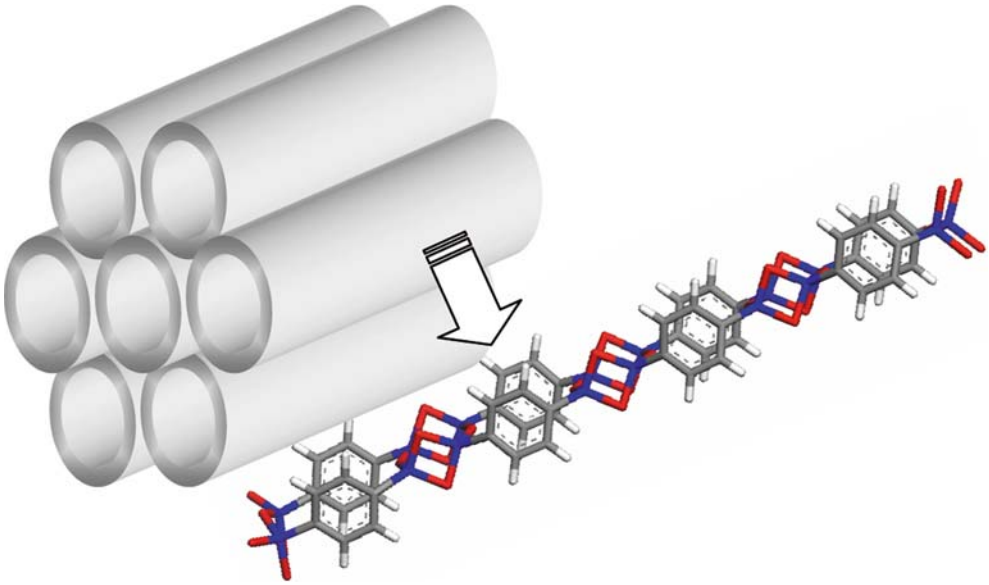

Figure 1. Representation of mesoporous benzene silica (MBS).

usefulness arises from the ability of the heme group to oxidize organic molecules using hydrogen peroxide. Unfortunately, free MP-11 has the tendency to aggregate in solution due to both intermolecular attraction and ligation through the metal center [73]. When MP-11 oligimerizes through coordination to the metal center, the heme becomes less accessible and the activity of the MP-11 is adversely affected. Immobilization in a suitable host material may prevent aggregation and render the heme more accessible to substrates. Previously, MP-11 has been immobilized on such supports as sol–gel silica glass [73], on gold [74], silver [75], and in reverse micelles [76]. We now report herein the immobilization of microperoxidase-11 in periodic mesoporous organosilica MBS and functionalized derivatives of MBS as well as in the 3-dimensional $[Cu(OOC–C_6H_4–C_6H_4–COO)\cdot ½\ C_6H_{12}N_2]_n$ metal organic framework. The percent conversion of Amplex® UltraRed and methylene blue to their respective oxidation products by the immobilized peroxidase MP-11 was evaluated.

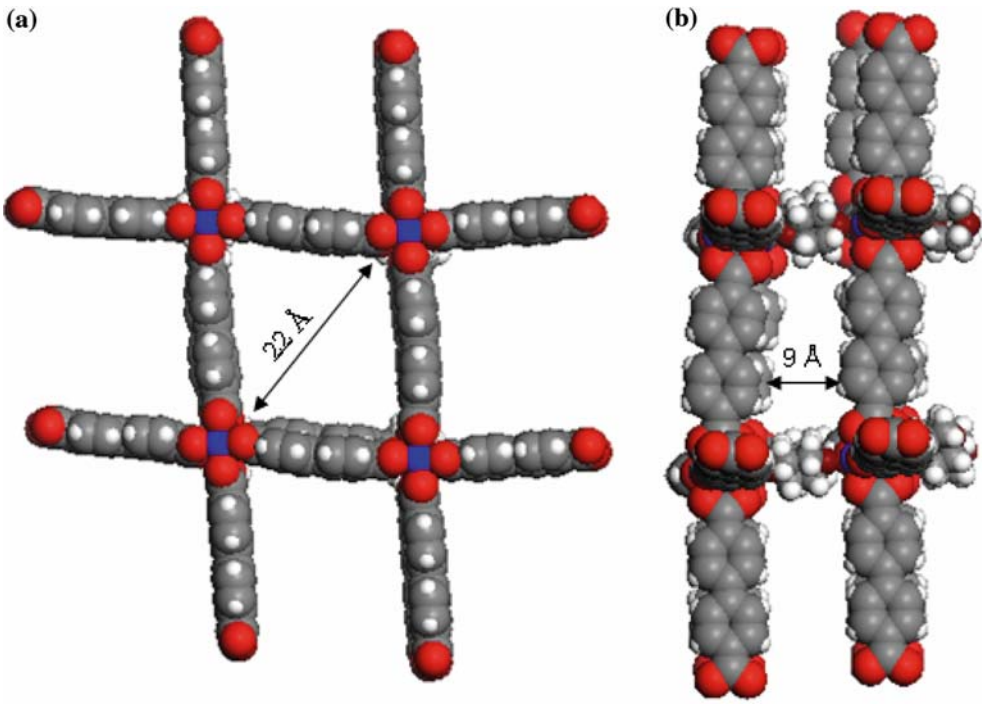

Figure 2. Structure of $Cu(OOC–C_6H_4–C_6H_4–COO)\ ½\ C_6H_{12}N_2]_n$ MOF, (a) front view and (b) side view calculated using Materials Studio.

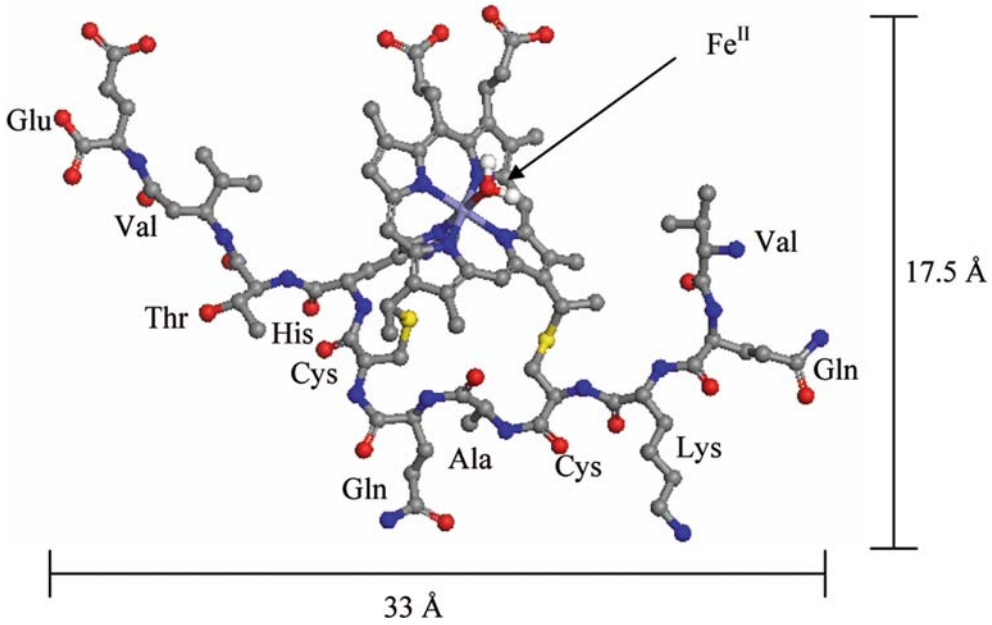

Figure 3. Microperoxidase-11 calculated using Materials Studio.

2. Experimental

2.1. MOF synthesis

The nanocrystalline MOF [Cu(OOC–C_6H_4–C_6H_4–COO) ½ $C_6H_{12}N_2$]$_n$ was synthesized by modifying the procedure reported by Seki *et al.* [71]. To form the MOF, a layered 2-D copper(II) dicarboxylate is synthesized and then pillared with 1,4-diazabicyclo[2.2.2]octane, in a 1:1 copper to pillar mole ratio, to form a 3-D structure. To synthesize the layered MOF, 0.59 g of copper(II) acetate (Fisher Scientific) was dissolved in 25 mL of ethanol (Aaper Alcohol and Chemical Company) and 0.25 g of 4,4′-biphenyldicarboxylic acid (Aldrich) was dissolved in 70 mL *N,N*-dimethylformamide (EM Science) and 0.30 mL formic acid (Aldrich). The solutions were mixed together with stirring and transferred to a 23 mL Teflon® lined autoclave. The reaction was heated at 50 °C for ~72 h. The reaction was removed from the oven and allowed to cool to room temperature. The mixture was then filtered and the blue solids were washed with ethanol. The collected solids were dried in a vacuum oven at 90 °C overnight. This material was then pillared by placing 100 mg of the blue powder in a 23 mL Teflon® lined autoclave along with 0.023 g of 1,4-Diazabicyclo[2.2.2]octane (DABCO) (Aldrich) dissolved in 5.0 mL of Toluene (Mallinckrodt). The autoclave was heated at 110 °C while rotating (20 rpm) for 6 h. The mixture was then suction filtered and the green solid was washed with ethanol and dried in a vacuum oven at 90 °C overnight.

After the intercalation of DABCO to produce the 3-dimensional [Cu(OOC–C_6H_4–C_6H_4–COO) ½ $C_6H_{12}N_2$]$_n$ MOF, the XRD pattern of the powder was in accordance with that reported in the literature [71]. The MOF had a Langmuir surface area of 1260 m^2/g and an average pore size of 17.8 Å based on N_2 adsorption From SEM (not shown) the particle size of the MOF was ~100 nm.

2.2. MBS synthesis

Five different MBS molecular sieve samples were prepared for this study and will be referred to as MBS-1, MBS-2, MBS-3, AP-MBS-1, and EDA-MBS-1. MBS-1 was prepared according to a published procedure [70] using octadecyltrimethylammonium chloride (ODTMAC) (TCI America, Inc.) as the template. Typically, 0.87 g of ODTMAC were dissolved in 27 mL of a 0.45 M aqueous NaOH solution in a polypropylene bottle. To this solution, 1 g of 1,4- (bistriethoxysilyl)benzene (BTEB) (Aldrich) was added with vigorous stirring, then sonicated for 15 min at room temperature. The white suspension was stirred at room temperature for 24 h followed by heating at 90 °C for 48 h. The white powder was isolated, washed with water and dried at 50 °C. A similar synthesis was used to produce aminopropyl functionalized MBS and ethylenediamine functionalized MBS. In a typical synthesis, 0.87 g of ODTMAC were dissolved in 27 mL of a 0.45 M aqueous NaOH solution in a polypropylene bottle. Then, 1 g of BTEB and 0.11 g of 3-aminopropyltrimethoxysilane (APTMS) (for AP-MBS), or 1 g of BTEB and 0.08 g of N-[3-(trimethoxysilyl)propyl]-ethylenediamine (EDA-TMS) (for EDA-MBS) were combined and added to the surfactant solution under vigorous stirring at room temperature. The gel was stirred at room temperature for 24 h followed by heating at 90 °C for 48 h. To prepare template free MBS, the as-synthesized solids were refluxed in an ethanol/HCl mixture (20/1 v/v) for 24 h. MBS-2 was prepared using vitamin E TPGS (α-tocopheryl polyethylene glycol 1000 succinate)

(Eastman Chemical Co.) as the template [77]. In a typical preparation, 1 g of BTEB was added to a solution containing 0.4 g of vitamin E TPGS, 11 mL of 1 M HCl, and 8. mL of ethanol under vigorous stirring. This gel was stirred for ~2 h at room temperature, then aged at 45 °C for ~20 h followed by heating at 90 °C for 48 h in a polypropylene bottle. MBS-3 was prepared according to a published procedure using Pluronic 123 (P123) block copolymer ($EO_{20}PO_{70}EO_{20}$) (BASF) as the structure-directing agent [78]. Initially, 1.1 g of P123 were dissolved in 1.4 mL of 2 M HCl and 41.5 mL of deionized water at room temperature. To this solution, 1.25 g of BTEB was added and the gel was stirred at 0 °C for 1 h, then at room temperature for 24 h followed by heating at 90 °C for 24 h in a polypropylene bottle. MBS-2 and MBS-3 powder were refluxed in ethanol for 24 h to remove the vitamin E TPGS and P123 templates respectively.

2.3. Immobilization of MP-11 in MOF

A 45 μM solution of MP-11 was prepared by dissolving 3.50 mg of MP-11(Aldrich) in 100 mL of *N, N*-dimethylformamide (EM Science). To immobilize the MP-11 10 mL of this solution was added to 10 mg of the MOF. The mixture was stirred at RT for 3 h. To isolate the MOF immobilized MP-11 the mixture was centrifuged and the supernatant was decanted. The supernatant was then filtered with a 0.2 μm syringe filter. The uptake of MP-11 was monitored by the disappearance of the Soret band (416 nm) in the supernatant.

2.4. Immobilization of MP-11 in MBS materials

A 100 μM stock solution of MP-11 was prepared by dissolving 9.34 mg MP-11 in 50.0 mL 50 μM potassium phosphate buffer at 7.24 pH. Desired concentrations were prepared by successive dilutions of the stock solution. To immobilize the enzyme 10.0 mL 20 μM MP-11 were added to 10.0 mg of mesoporous support and left stirring overnight (> 18 h) at room temperature. The suspension was then centrifuged for 15 min in order to collect the immobilized enzyme. The supernatant was collected to determine the enzyme's uptake by monitoring the Soret band at 404 nm. The solid left in the test tube was rinsed with fresh buffer and centrifuged for 15 more minutes. The supernatant was removed and the solid was saved for the determination of percent conversion.

2.5. Assays

2.5.1. MOF

A 4.5 μM solution of methylene blue (Allied Chemical) was prepared by dissolving 9.8 mg of methylene blue in 250 mL of DMF, this solution was successively diluted until the desired concentration was obtained. For the oxidation, 5 mL of 2.4 μM methylene blue was added to 10 mg MOF/MP-11 and 10 μL 30% hydrogen peroxide. This mixture was stirred for 1 h at RT and then separated via centrifugation. Also, a control reaction in which 5.0 mL 20 μM DMF solution of free MP-11 was reacted with 10 μL 30% hydrogen peroxide and 2.4 μM methylene blue under the same conditions as above, was performed. Also, a control reaction was performed with 10 mg as-synthesized MOF, 10 μL 30% hydrogen peroxide, and 5 mL of 2.4 μM methylene blue in DMF. The progress of the reactions were monitored by the disappearance of the visible band at 664 nm associated with methylene blue.

2.5.2. MBS materials

A colorimetric assay was employed to determine the MP-11's ability to oxidize Amplex® UltraRed. Amplex® UltraRed reagent (10-acetyl-3,7-dihydroxyphenoxazine) reacts in a 1:1 stoichiometric ratio with H_2O_2 producing resorufin ($C_{12}H_7NO_3$), a red fluorescent product easily detected with a UV spectrophotometer [79]. In general, 5.0 mL 50 μM Amplex UltraRed and 5.0 mL 50 μM H_2O_2 were added to test tube containing immobilized MP-11 in 10.0 mg of mesoporous support. Samples were quickly placed in orbital shaker at 70 rpm and the reaction was allowed to run for 60 min. Test tubes were then placed in centrifuge for 15 min. The supernatant was collected to determine the amount of resorufin produced by monitoring its absorbance at 568 nm.

2.6. Instrumentation

Powder X-ray diffraction patterns were obtained using a Scintag XDS 2000 X-ray diffractometer using CuKα radiation. Infrared spectra were acquired from KBr pellets with a Nicolet Avatar 360 FT-IR spectrophotometer with a resolution of 4 cm^{-1}. Samples for scanning electron microscopy were coated with Pd/Au and micrographs obtained on a Leo 1530 VP electron microscope. Nitrogen adsorption was measured at 77 K on a Quantachrome Autosorb 1. All samples were outgassed at 100 °C and 10^{-6} torr prior to measurements. A seven point BET equation was used to calculate surface areas. Pore size distribution was calculated from the desorption data using the BJH method. UV–Vis spectra were collected using Shimadzu UV-1601PC spectrophotometer.

3. Results and discussion

3.1. Immobilization of MP-11 in MBS materials

Five types of mesoporous benzene silica (MBS) molecular sieves were prepared for this study. MBS samples were prepared with the 1,4-benzene bridged silane (BTEB) as described in the experimental section. Powder XRD patterns of the hybrid MBS-1 (not shown) and MBS-3 (figure 4c) hybrid materials confirm a

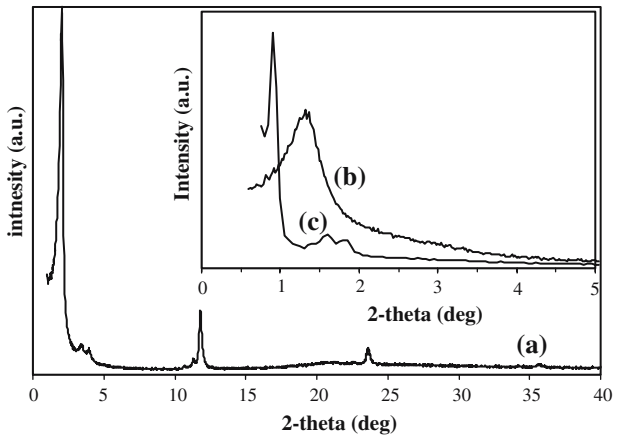

Figure 4. Powder XRD of template extracted (a) AP-MBS, (b) MBS-2, and (c) MBS-3.

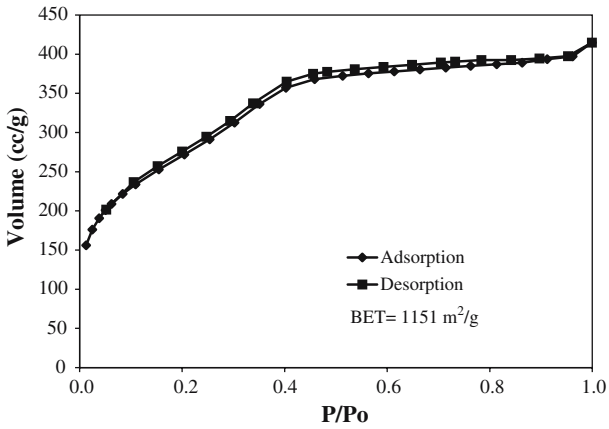

Figure 5. N_2 adsorption Isotherm and BET surface area of MBS-2.

typical well-ordered hexagonal mesoporous material with d_{100} spacing of ~4.57 and 8.71 nm respectively. The former is consistent with the MBS material prepared by Inagaki and co-workers, which exhibited a d_{100} spacing of 4.55 nm [70]. The XRD patterns for the MBS-2 hybrid (figure 4b) indicate the presence of a disordered mesoporous structure as evidenced by the broad low angle peak (d_{100} spacing ~6.07). The XRD patterns for MBS-1 (not shown), AP-MBS (figure 4a), and EDA-MBS (not shown) are quite different from the normal hexagonally arranged mesoporous material. The patterns display three low angle reflection peaks corresponding to the 100, 110 and 200 reflections suggesting a well-ordered structure. Additionally, the XRD patterns also display higher angle reflections at d-spacings of 7.6, 3.8 and 2.5 A respectively. These higher angle reflections are due to molecular-scale periodicity in the PMO pore walls along the channel direction. [70], which can be attributed to the homogeneous distribution of the phenyl groups at the molecular level. The surface area, pore size and pore volume, determined from the nitrogen adsorption/desorption isotherms of the hybrid mesoporous materials are summarized in table 2. All five mesoporous hybrids in this study display a type IV isotherm. Figure 5 shows the nitrogen isotherm for EDA-MBS. The isotherm is typical of MBS hybrids prepared under basic conditions using ODTMAC as template. MBS-2 also displays similar isotherms. In contrast, the MBS-3 isotherm presents a large hysterisis and capillary condensation of nitrogen occurs at higher partial pressure ($P/P_o \sim 0.6$), which indicates that this structure is composed of larger mesopores. The BJH pore size distribution calculated from the desorption branch for the mesoporous hybrids is shown in table 2. The mesoporous hybrids have fairly narrow pore size distribution with pore sizes of 2.7 to 3 nm for MBS-1, MBS-2, AP-MBS, and EDA-MBS. MBS-3 on the other hand has mesopores in the 5.5 nm range. MBS-1, MBS-2, and EDA-MBS show high surface area in the range of 950–1150 m^2/g, while the surface area MBS-3 and AP-MBS surface area was smaller at ~615–630 m^2/g. The MBS material prepared by Inagaki *et al.* [70] exhibits a larger pore size of 3.8 nm and a smaller surface area of 818 m^2/g when compared to the MBS-1 material prepared for this study. These differences are accounted for

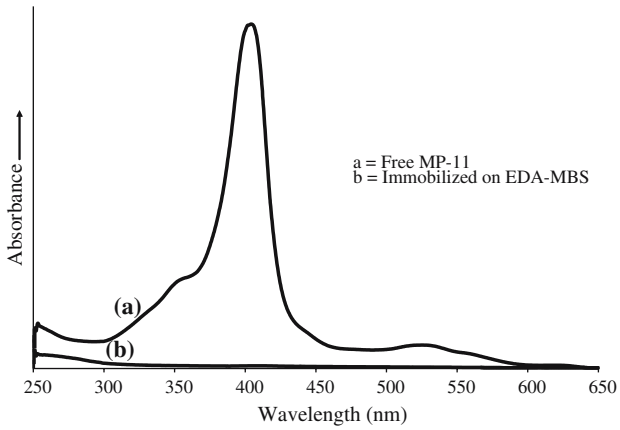

Figure 6. UV–Vis spectra of MP-11 solution before and after immobilization.

Table 2
Mesoporous support pore size and the corresponding MP-11 uptake

	MBS-1	MBS-2	MBS-3	AP-MBS	EDA-MBS
Pore size (Å)	27	30.5	55	26.6	27
Surface Area (m^2/g)	956	1151	631	615	918
Uptake (μmol/g support)	20 ± 1	17.1 ± 0.2	19.0 ± 0.9	19.4 ± 0.8	18.45 ± 0.06
Percent	98 ± 2	86 ± 2	98 ± 1	99.3 ± 0.6	99.6 ± 0.3

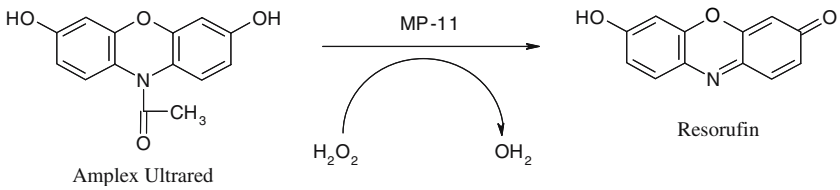

Figure 7. Reaction scheme for the oxidation of Amplex® UltraRed to resorufin.

based on the type of analysis carried out, where the BJH and the modified BJH analysis [80] give different pore diameters. Additionally, differences in surface area can arise from variations in the preparative technique.

MP-11 (pI = 4.7 [81]) was immobilized in all MBS supports by adsorption from solution. Van der waals interactions between the MP-11 and the curved pore walls of the MBS materials may facilitate this process. A representative UV-Vis spectrum showing the buffer solution before and after immobilization of MP-11 on EDA-MBS is shown in figure 6. The disappearance of MP-11 characteristic Soret band at 404 nm is observed, when the supernatant after immobilization was analyzed. The uptake of the MP-11 by all MBS supports is shown in table 2. The lowest loading was 86 ± 2% for MBS 2 and the highest loading was 99.6 ± 0.3% for EDA-MBS. In most cases the loadings were ≥98% The MP-11 is ~17.5×33 Å in size such that it will readily fit in all the supports. MBS-1 and MBS-2 have similar pore sizes and surface areas so it is not clear why there is a small difference in MP-11 uptake. The MBS-2 has thicker pore walls (36 vs 25 Å) and as a result the phenyl bridges in the pores walls are less ordered. This may be a factor in the adsorption of MP-11. The highest loadings were obtained with the MBS materials that have pendent amine groups. In this case, the amine groups may interact with the MP-11 facilitating uptake.

3.2. Oxidation of Amplex® UltraRed

The ability of the immobilized MP-11 to oxidize Amplex® UltraRed to Resorufin in the presence of H_2O_2 [82] was determined by a colorimetric assay, as shown in figure 7. The reaction was followed by UV–Vis spectroscopy. A representative UV–Vis spectrum showing the disappearance of Amplex® UltraRed concurrent with the appearance of Resorufin is shown in figure 8. A control reaction comprising 5.0 mL 50 μM Amplex® UltraRed, 5.0 mL 50 μM H_2O_2 and 5.0 mL 20 μM MP-11 was run in order to compare free MP-11 to the immobilized MP-11. The percent conversion after 1 h is shown in figure 9. The immobilized peroxidase, compared to the free peroxidase, exhibit a lower percent conversion. The lowest conversion of 8.1 ± 0.4% was obtained when immobilized in MBS-1 followed by 10 ± 3% in AP-MBS and 16 ± 5 in EDA-MBS. The MBS-2 and MBS-3 supports exhibited a 29 ± 1% and 35 ± 8%, respectively. Higher conversions were obtained with either lower loadings, as in the case of MBS-2 or in larger pore sized materials, as in the case of MBS-3 (table 2). The one dimensional pores of the MBS materials may limit access the MP-11. This is consistent with higher activity in larger pore sized materials, where the peroxidase, 17.5×33 Å, is not constrained in terms of orientation in the pore.

The MP-11 peroxidase was stable to leaching in most MBS supports. However, in the case of the larger pore size MBS-3 material some leaching occurred during the assay. This is consistent with the findings of Takahashi and co-workers who reported a direct relationship between increasing pore size and susceptibility to leaching out to solution [50]. Additionally, a larger error was reported for this material and it was estimated that 5% conversion of the total reported was attributed to the free enzyme found in solution after the assay.

3.3. Immobilization of MP-11 in MOF

The size of MP-11 (figure 3) (~17.5×33 Å) is such that a specific orientation of the protein is required to fit. MP-11 was adsorbed into the MOF by stirring in a solution at RT. The amount adsorbed was monitored by UV-Vis spectroscopy. As can be seen in figure 10 the MOF adsorbed ~67% of the MP-11 from the solution. The loading of MP-11 in the MOF was calculated to be 30 μmol/g. This is lower than the MBS materials but the pores are smaller. The Langmuir surface area after adsorption of MP-11 was 300 m^2/g, representing a 76% decrease.

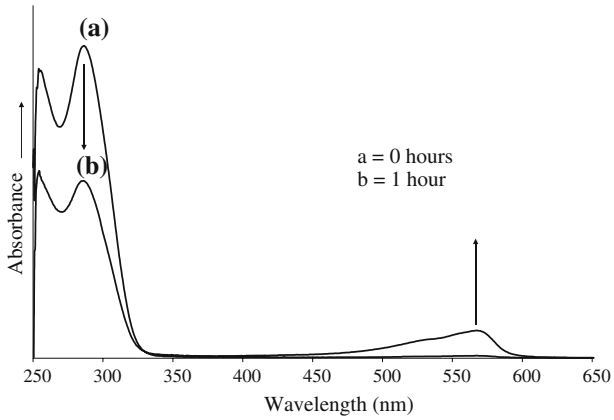

Figure 8. UV–Vis spectra of the oxidation of Amplex® UltraRed to resorufin.

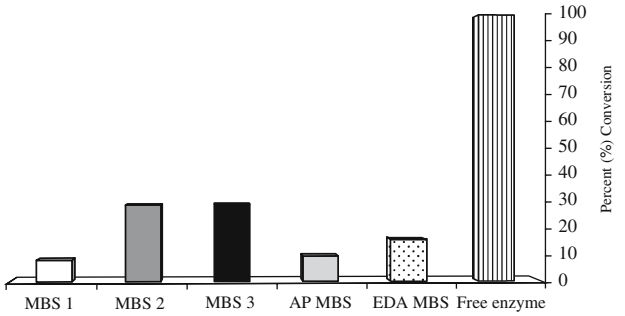

Figure 9. Percent conversion of Amplex® UltraRed to resorufin using 5.0 mL 50 μM Amplex® UltraRed, 5.0 mL 50 μM H_2O_2 and either free or immobilized MP-11.

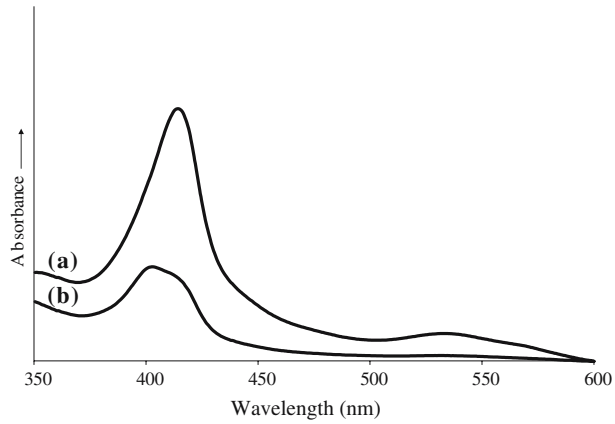

Figure 10. UV–Vis spectra for MOF uptake of MP-11, (a) before and (b) after immobilization.

To determine if the peroxidase would leach out of the MOF after immobilization, the MOF immobilized MP-11 was stirred at room temperature for 72 h in DMF. The UV-Vis of the supernatant showed no MP-11 in solution.

3.4. Oxidation of methylene blue

The oxidative ability of the CuMOF immobilized MP-11 was evaluated by monitoring the oxidation of methylene blue (figure 11). The progress of the reactions was monitored by UV-Vis spectroscopy using the absorbance band at 664 nm. The reactions were performed at room temperature in DMF. The reaction was stopped after 1 h and the supernatant was isolated by centrifugation. This solution was added to the MOF immobilized MP-11 along with hydrogen peroxide and allowed to react at room temperature. After 1 h the supernatant was isolated by centrifugation and analyzed by UV–Vis. The starting concentration of the methylene blue solution was 2.35 μM and after reaction with MOF immobilized MP-11 the concentration was reduced to 0.87 μM, corresponding to 63 ± 5.1% conversion (figure 12). A control reaction, in which a DMF solution of free MP-11 was reacted with hydrogen peroxide and methylene blue under the same conditions as before, was performed. This reaction showed only a 6 ± 5.2% percent conversion of methylene blue. Also, because the MOF is a porous material and has the ability to absorb various species a control reaction was performed with as-synthesized MOF, hydrogen peroxide, and methylene blue in DMF. After the mixture was stirred at room temperature for 1 h there was no change in the concentration of methylene blue.

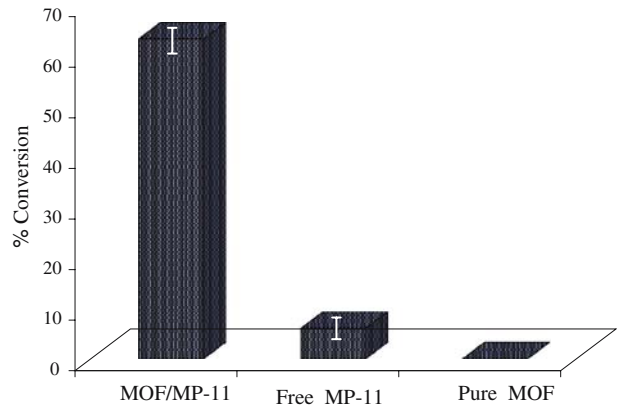

Figure 12. The percent conversion of methylene blue by (a) MOF immobilized MP-11, (b) free MP-11, and (c) pure MOF from a solution of 2.35 μM methylene blue, and 10 μL 30% H_2O_2.

4. Conclusions

The physical immobilization of microperoxidase-11 in copper(II) dicarboxylate metal organic framework

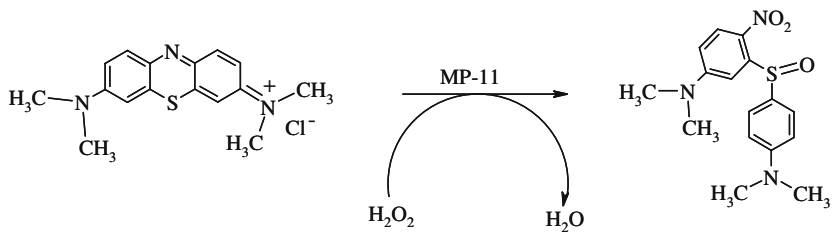

Figure 11. Reaction scheme for the oxidation of methylene blue.

and periodic mesoporous organosilicas has been demonstrated. The peroxidase retains activity and, in the case of methylene blue bleaching, the supported MP-11 is considerably more active. This holds promise for the application of this catalyst in organic solvents. The one dimensional mesoporous benzene silicas exhibit lower conversion but this is consistent with most of the examples in table 1. However, the hybrid frameworks of PMO materials also hold promise for applications in organic solvents. Current efforts are directed at synthesizing PMOs and MOFs that could potentially operate in concert with immobilized enzymes to create hybrid catalysts. Thus one may be able to use the host matrix as a co-factor or co-catalyst.

Acknowledgments

We thank the Robert A. Welch Foundation for support of this project.

References

[1] D.E. De Vos, B.F. Sels and P.A. Jacobs, CATTECH 6 (2002) 14.
[2] A. Wiseman, J. Chem. Tech. Biotech. 65 (1996) 3.
[3] B.M. Weckhuysen, A.A. Verberckmoes, I.P. Vannijvel, J.A. Pelgrims, P.L. Buskens, P.A. Jacobs and R.A. Schoonheydt, Ang. Chem. Int. Ed. 34 (1996) 2652.
[4] M.E. Davis, A. Katz and W.R. Ahmad, Chem. Mat. 8 (1996) 1820.
[5] R. Robert and P. Ratnasamy, J. Mol. Cat. A 100 (1995) 93.
[6] D.R. Corbin and N. Herron, J. Mol. Cat. 86 (1994) 343.
[7] J.M. Thomas, R. Raja, G. Sankar and R.G. Bell, Acc. Chem. Res. 34 (2001) 191.
[8] K.J. Balkus Jr., A.K. Khanmamedova, K.M. Dixon and R. Bedioui, Appl. Cat. A 143 (1996) 159.
[9] G. Gbery, A. Zsigmond and K.J. Balkus Jr., Cat. Lett. 74 (2001) 77.
[10] A.G. Gabrielov, K.J. Balkus Jr., S.L. Bell, F. Bedioui and J. Devynck, Micropor. Mater. 2 (1994) 119.
[11] K.J. Balkus Jr, A.G. Gabrielov, S.L. Bell, F. Bedioui and L. Roue, Inorg. Chem. 33 (1994) 67.
[12] K.J. Balkus Jr., M. Eissa and R. Levado, J. Am. Chem. Soc. 117 (1995) 10753.
[13] A.X. Yan, X.W. Li and Y.H. Ye, Appl. Biochem. Biotechnol. 101 (2002) 113.
[14] J. Diaz and K.J. Balkus Jr, J. Mol. Cat. B: Enz. 2 (1996) 115.
[15] L. Washmon-Kriel, V.L. Jimenez and K.J. Balkus Jr., J. Mol. Cat. B 10 (2000) 453.
[16] Y. Wei, J. Xu, Q. Feng, M. Lin, H. Dong, W. J. Zhang and C. Wang, J. Nanosci. Nanotechnol. 1 (2001) 83.
[17] Q. Feng, J. Xu, M. Lin, H. Dong and Y. Wei, Poly. Mater. Sci. Eng. 83 (2000) 502.
[18] Y. Wei, J. Xu, Q. Feng, H. Dong and M Lin, Mater. Lett. 44 (2000) 6.
[19] Y. Wei and K.Y. Qiu, Chin. J. Polym. Sci. 18 (2000) 1.
[20] H.M. Mody, K.H. Mody, R.V. Jasra, H.J. Shin and R. Ryong, Indian J. Chem. A. 41 (2002) 1795.
[21] P.H. Pandya, R.V. Jasra, B.L. Newalkar and P.N. Bhatt, Micropor. Mesopor. Mater. 77 (2004) 67.
[22] A. Macario, V. Calabro, S. Curcio, M. De Paola, G. Giordano and G. Iorio, A. Katovic Stud. Surf. Sci. Cata. 142B (2002) 1561.
[23] C.H. Lee, S.T. Wong, T.S. Lin and C.Y. Mou, J. Phys. Chem. B 109 (2005) 775.
[24] Y. Wang and F. Caruso, Adv. Funct. Mater. 14 (2004) 1012; Y. Wang and F. Caruso, Chem. Comm. 13 (2004) 1528.
[25] E. Dumitriu, F. Secundo, J. Patarin and I. Fechete, J. Mol. Catal. B: Enzym 22 (2003) 119.
[26] A. Borole, S. Dai, C.L. Cheng, M. Rodriguez Jr. and B.H. Davison, Appl. Biochem. Biotechnol. 113–116 (2004) 273.
[27] Y.J. Han, J.T. Watson, G.D. Stucky and A. Butler, J. Mol. Catal. B: Enzym. 17 (2002) 1.
[28] N.W. Fadnavis, V. Bhaskar, M.L. Kantam and B.M. Choudary, Biotechnol. Prog. 19 (2003) 346.
[29] J. Deere, E. Magner, J.G. Wall and B.K. Hodnett, Biotechnol. Prog. 19 (2003) 1238.
[30] J. Deere, E. Magner, J.G. Wall and B.K. Hodnett, Catal. Lett. 85 (2003) 19.
[31] X. Xu, B. Tian, J. Kong, S. Zhang, B. Liu and D. Zhao, Adv. Mater. 15 (2003) 1932.
[32] J. Deere, E. Magner, J.G. Wall and B.K. Hodnett, J. Phys. Chem. B 106 (2002) 7340.
[33] J. Deere, E. Magner, J.G. Wall and B.K. Hodnett, Stud. Surf. Cata. 135 (2001) 3694.
[34] J. Deere, E. Magner, J.G. Wall and B.K. Hodnett, Chem. Commun. 5 (2001) 465.
[35] L. Washmon-Kriel, V.L. Jimenez and J. Balkus Jr, J. Mol. Catal. B Enzym. 10 (2000) 453.
[36] M.E. Gimon-Kinsel, V.L. Jimenez, L. Washmon and J. Balkus Jr, Stud. Surf. Cat. 117 (1998) 373.
[37] L. Washmon-Kriel, V.L. Jimenez and J. Balkus Jr, J. Mol. Catal. B: Enzym 10 (2000) 453.
[38] N. Nobuyoshi, I. Kohji, S. Manabu, N. Takashi and T. Hideaki, Biosci. Biotechnol. Biochem 66 (2002) 2739.
[39] T. Coradin and J. Livage, C. R. Chim. 6 (2003) 147–152.
[40] T. Itoh, N. Ouchi, Y. Nishimura, H.S. Hui, N. Katada, M. Niwa and M. Onaka, Green Chem. 5 (2003) 494.
[41] Z.V. Smelaya and Y.G. Goltsov, Khimiya, Fiz. ta Tekhnologiya Poverkhni 7–8 (2002) 134.
[42] B. Liu, R. Hu and J. Deng, in: *Analyst* (Cambridge, UK) 122 (8) 821; H. Dong, J. Xu, Q. Feng and Y. Wei, Poly. Mater. Sci. Eng. 83 (2000) 504–505.
[43] Y. Wei, H. Dong, J. Xu and Q. Feng, Chem. Phys. Chem. 3 (2002) 802.
[44] H. Dong, J. Xu, Q. Feng and Y. Wei, Poly. Mater. Sci. Eng. 83 (2000) 504.
[45] Z. Dai, S. Liu, H. Ju and H. Chen, Biosens. Bioelectron. 19 (2004) 861.
[46] H. Takahashi, B. Li, T. Sasaki, C. Miyazaki, T. Kajino and S. Inagaki, Microporous Mesoporous Mater. 44–45 (2001) 755.
[47] B. Li, S. Inagaki, C. Miyazaki and H. Takahashi, Chem. Res. Chin. Univ. 18 (2002) 200.
[48] B. Li and H. Takahashi, Biotechnol. Lett. 22 (2000) 1953.
[49] B. Li, S. Inagaki, C. Miyazaki and H. Takahashi, Cailiao Yanjiu Xuebao 14 (2000) 625.
[50] H. Takahashi, B. Li, T. Sasaki, C. Miyazaki, T. Kajino and S. Inagaki, Chem. Mater. 12 (2000) 3301.
[51] K. Katsuya, I. Roxana, S. Takao, Y. Yoshiyuki and T. Haruo, Biosci. Biotechnol. Biochem. 67 (2003) 203.
[52] H. Ma, J. He, D.G. Evans and X. Duan, J. Mol. Catal. B: Enzym. 30 (2004) 209.
[53] R.M. Blanco, P. Terreros, M. Fernandez-Perez, C. Otero and G. Diaz-Gonzalez, J. Mol. Catal. B: Enzym. 30 (2004) 83.
[54] E. Dumitriu, F. Secundo, J. Patarin and I. Fechete, J. Mol. Catal. B: Enzym. 22 (2003) 119.
[55] G. Kuncova, J. Szilva, J. Hetflejs and S. Sabata, J. Sol-Gel Sci. Technol. 26 (2003) 1183.
[56] A. Vinu, V. Murugesan and M. Hartmann, J. Phys. Chem. B 108 (2004) 7323.

[57] J. Lei, J. Fan, C. Yu, L. Zhang, T. B. Jiang and D. Zhao, Micropor. Mesopor. Mater. 73 (2004) 121.
[58] J.M. Kisler, G.W. Stevens and A.J. O'Connor, Mater. Phy. Mech. 4 (2001) 89.
[59] J. Fan, J. Lei, L. Wang, C. Yu, B. Tu and D. Zhao, Chem. Comm. 17 (2003) 2140.
[60] H. Takahashi and C. Miyazaki, Toyota Chuo Kenkyusho R&D Rebyu 37 (2002) 61.
[61] Knops-Gerrits and H.J.M. W.A. Peter-Paul Goddard, Catal. Today 81 (2003) 263.
[62] Z. Dai, X. Xu and H. Ju, Anal. Biochem. 332 (2004) 23; Z.V. Smelaya and Y.G. Goltsov Khimiya, Fiz. ta Tekhnologiya Poverkhni 7–8 (2002) 134.
[63] C. Lei, Y. Shin, J. Liu and E.J. Ackerman, J. Am. Chem. Soc. 124 (2002) 11242.
[64] A. Chong, S. Maria and X.S. Zhao, Catal. Today 93–95 (2004) 293.
[65] J. He, X. Li, D.G. Evans, X. Duan and C. Li, J. Mol. Catal. B: Enzym 11 (2000) 45.
[66] R. Revanur, S. Zhao, G. Hermann and W.R. Germany, J. Am. Chem. Soc. 126 (2004) 12224.
[67] H.H.P. Yiu, P.A. Wright and N.P. Botting, J. Mol. Catal. B Enzym 15 (2001) 81.
[68] H.H.P. Yiu, P.A. Wright and N.P. Botting, Micropor. Mesopor. Mater. 44–45 (2001) 763.
[69] B. Hatton, K. Landskron, W. Whitnall, D. Perovic and G.A. Ozin, Acc. Chem. Res. 38 (2005) 305.
[70] S. Inagaki, S. Guan, T. Ohsuna and O. Terasaki, Nature 416 (2002) 304.
[71] K. Seki and W. Mori, J. Phys. Chem. B 106 (2002) 1380.
[72] J.L.C. Roswell and O.M. Yaghi, Micropor. Mesopor. Mater. 73 (2004) 3.
[73] E.N. Kadnikova and N.M Kostic, J. Org. Chem. 68 (2003) 2600.
[74] Y. Astuti, E. Topoglidis, G. Gilardi and J.R. Durrant, Bioelectrochem. 63 (2004) 55.
[75] F. Wang, J. Zheng, X. Li, Y. Ji, Y. Gao, W. Xing and T. Lu, J. Electro. Chem. 545 (2003) 123.
[76] S. Okazaki, S. Nagasawa, M. Goto, S. Furusaki, H. Wariishi and H Tanaka, Biochem. Eng. J. 12 (2002) 237.
[77] D.H. Coutinho, B. Gorman and K.J. Balkus, Jr., Micropor. Mesopor. Mater. 91 (2006) 276.
[78] Y. Goto and S. Inagaki, Chem. Commun. (2002) 2410.
[79] M. Zhou, Z. Diwi, N. Panchuk-Voloshina and R.P. Haugland, Anal. Biochem. 253 (1997) 162.
[80] M. Kruk and M. Jaroniec, Chem. Mater. 13 (2001) 3169.
[81] N. Huang, Z. Zhang, X. Han, J. Tang, Z. Peng, S. Dong and E. Wang, Biophysical Chemistry 94 (2001) 165.
[82] I. Pastor, R. Esquembre, V. Micol, R. Mallavia and C. Reyes Mateo, Anal. Biochem. 334 (2004) 335.